

DYNAMIC ACTIVATION OF STRUCTURAL THERMAL MASS IN A MULTI-ZONAL BUILDING WITH DUE REGARD TO THERMAL COMFORT

Henryk Wolisz, Pascal Block, Rita Streblov, Dirk Müller
RWTH Aachen University, E.ON Energy Research Center
Institute for Energy Efficient Buildings and Indoor Climate
52074 Aachen, Germany
hwolisz@eonerc.rwth-aachen.de

ABSTRACT

The following analysis faces the challenge of matching the availability of renewable energies with the heating demand of a residential one-family house through demand side management. Depending on the availability signal of excess renewable electricity generation, the building's structural thermal mass is activated through the heating system. Thereby, the air temperatures in different building zones are dynamically controlled according to the type of the zone, the current and the expected occupancy.

It is shown that the share of the energy demand covered during periods of excess renewable energy can be more than doubled, yet causing some potential comfort violations. However, the presented multi-zone control algorithm with occupancy and building behaviour forecasting can distinctly reduce the occurring comfort violations, while just slightly reducing the storage potential.

INTRODUCTION

With the growing share of renewable non-dispatchable energy generation, the challenge arises to match electricity production and consumption. Residential and commercial buildings, which account for up to 30 % of Germany's final-energy consumption (BMWi, 2013), have increasingly more electricity-based heating systems (e.g. heat pumps) and could therefore provide consumption flexibility to balance the fluctuating electricity supply. In particular, excess electric energy from renewable energy generation could be efficiently stored as thermal energy within residential buildings.

In Building Simulation 2013, we presented the concept of storing energy directly in the building's structural thermal mass (Wolisz, 2013). Based on simulations with a single thermal zone and predefined set-temperature steps, the concept demonstrated promising potential. Therefore, a distinctly extended dynamic Demand Side Management (DSM) approach for sensible heat storage in a multi-zone residential building is presented in this work. In comparison to the study performed in 2013, which was focusing on the detailed energy flows within the building structures, this analysis evaluates the impact of different complexities of DSM control algorithms upon the

building activation. Depending on an availability signal of excess electricity generation from renewable energy sources, the air set-temperatures within the building are adapted. To use the storage capacity of the building's thermal mass effectively and maximise the amount of stored thermal energy, the temperatures in different building zones are independently increased when renewable energy is available and reduced if not. As a result, the building's thermal mass is dynamically activated through the increased radiation on one hand and through the increased air temperature on the other hand. Simultaneously, taking the occupancy of the building into account, the control algorithm attempts to ensure that the thermal comfort of residents is not violated. Therefore, comfort conditions and threshold values (i.e. constraints) for the dynamic control approach are taken from literature (Peeters, 2009). Based on those constraints, a rule-based control algorithm utilizing state machines has been implemented in Modelica / Dymola (Modelica Association, 2014). The major advantage of this algorithm is the good ratio of simplicity and efficiency. Thus, it could be implemented in an existing building application without much effort, as it only requires a few input parameters and electronic control of heating valves. Further, detailed information about the heating system is not required.

MODELLING AND APPROACH

The focus of this analysis is the investigation of the thermal mass activation algorithm and its dynamic behaviour, particularly regarding the distinctions between the single- and the multi-zone control approaches. For the simulation of the different thermal zones, a simplified building model developed by Lauster (Lauster, 2014) and based on the Guideline VDI 6007 (VDI, 2012) is used. Lauster's model was mostly used for city district simulations in the past. However, the calculations schemes used in his model are improved in comparison with the underlying guideline, which is designed for calculation of the transient thermal response of single rooms and buildings. The used model allows analysing and comparing different control approaches, keeping reasonable computation times while still getting profound results for the thermal behaviour within the building zones.

According to VDI 6007, the thermal behaviour of a building can be described through interconnection of resistances and capacities in analogy to an electrical circuit. Here, the model aggregates all exterior building components such as walls, windows, and the roof into one “outer wall” building component with asymmetrical thermal load. Accordingly, all interior building components where the load on the two surfaces is symmetrical are aggregated to one “inner wall” component. Based on the same procedure, we have also implemented a model with three different building zones. Thereby, bathrooms, bedrooms, and all other rooms are distinguished and modelled separately with the associated shares of “inner” and “outer walls”. For all zones, the “inner wall” component is considered adiabatic and it reacts to heat exposure like a thermal storage, thus being represented by one resistance and one capacitance. In contrast, the “outer wall” contributes to the heat transfer and exchanges energy with the surrounding. In this case, two resistances and one capacitance represent the “outer wall”.

Besides the “inner-“ and “outer wall” objects, the model includes functions that represent all the necessary thermal processes inside a thermal zone. These are primarily radiative and convective heat exchange. In addition to that and as improvement of the guideline VDI 6007, the used building model takes also the heat capacity of the air into account. Furthermore, it applies the Stefan-Boltzmann law for the calculation of the radiative heat exchange instead of the linearized approach used in the VDI 6007. This is even more accurate and for example a crucial aspect for precise estimations of surface and operative temperatures within a room.

Heat exchange of the “outer wall” components with the environment (e.g. solar radiation) is incorporated by using an averaged “equal air temperature”. This temperature considers the short- and the long-wave radiation on differently oriented surfaces, the temperature of the ground, and the outdoor air temperature. The solar gain through the windows is considered additionally as radiative heat flow. Hence, equal air temperature and solar radiation are external loads. In accordance with VDI 6007, we consider the heating system with 50 % radiant and 50 % convective heat flow. The heating system itself is not further specified or simulated, as our focus is on the control approach. Therefore, the required heat is delivered by an ideal heat source with the nominal heating power required for the connected zone as calculated based on DIN 12831 (DIN, 2012). Further internal loads, such as the heat emission of persons, machines and lighting are also integrated directly as convective or radiative heat sources, whereby the convective share is 50 % for lighting and occupants and 60 % for machines. Ventilation is considered as an additional convective heat sink.

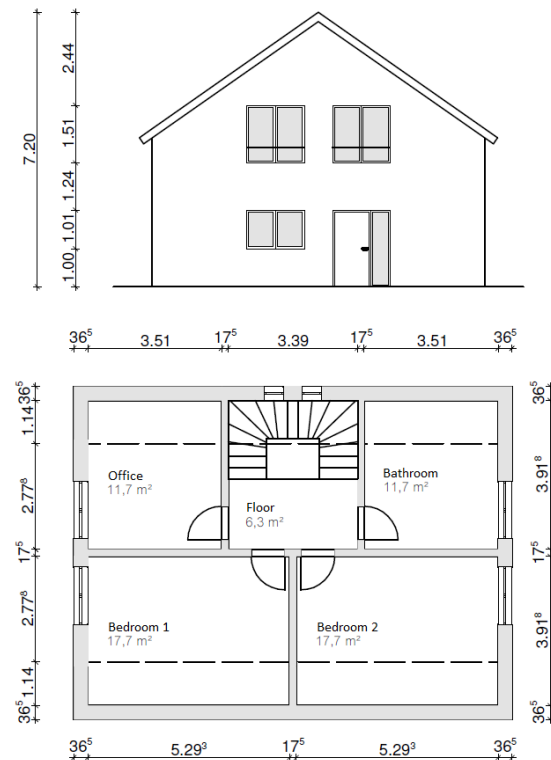


Figure 1

Top: Sketch of the modelled building from the east
Bottom: Layout of the first floor.

The modelled building is a one family house with 145 m² heated floor area. Figure 1 presents a sketch of the building from the east and the layout of the first floor. For the multi-zone control scenario, 11 % of the building’s floor area is considered bath- and sanitary rooms, 25 % is considered bedrooms, and the residual of 64 % is aggregated as other rooms. Table 1 gives the properties of the building’s envelope.

Table 1

Properties of the building envelope

in m ²	north	east	south	west
outer wall	40	39	37	37.5
windows	3	9	6	10.5

For this analysis, the occupation of the building is chosen considering the lifestyle of a working couple, where both adults work full time. The chosen occupation profiles of the building and the single building zones are given in Table 2.

Table 2

Occupation profiles for all building zones

	occupied	unoccupied
1-zone building	5 pm - 7:30 am	7:30 am - 5 pm
bedrooms	10 pm - 6 am	6 am - 10 pm
bathrooms	/	all day
other rooms	5 pm - 7:30 am	7:30 am - 5 pm

One crucial part of the presented approach is the consideration of thermal comfort, since severe violations of these conditions would undermine the acceptability of the suggested building operation. Therefore, limits for minimum and maximum comfort temperatures are chosen for every building zone. For this purpose the approach of (Peeters, 2009), who presents comfort values and scales for building energy simulation, and the DIN EN ISO standard 7730 (DIN, 2006) are used. As a first step, equations for the neutral temperature ϑ_n of the three thermal zones (bathroom, bedroom and other rooms) are derived. The neutral temperature ϑ_n is the air temperature of each building zone for which the human body reaches thermal balance with the surrounding. This temperature is dependent of the outside air temperature ϑ_{amb} and is acceptable for 90 % of the people according to Peeters. As an excerpt of Peeter’s approach equations (1.1) and (1.2) show the neutral temperature ϑ_n for bedrooms and equation (1.3) shows ϑ_n for the “other rooms”.

Bedrooms:

$$\vartheta_n = 16 \text{ }^\circ\text{C} \quad \text{for} \quad \vartheta_{amb} < 0 \text{ }^\circ\text{C} \quad (1.1)$$

$$\vartheta_n = 0.23 \times \vartheta_{amb} + 16 \text{ }^\circ\text{C} \quad \text{for} \quad \vartheta_{amb} \leq 12.6 \text{ }^\circ\text{C} \quad (1.2)$$

“Other rooms”:

$$\vartheta_n = 0.06 \times \vartheta_{amb} + 20.4 \text{ }^\circ\text{C} \quad \text{for} \quad \vartheta_{amb} < 12.5 \text{ }^\circ\text{C} \quad (1.3)$$

The thermal boundary conditions for the algorithm are chosen based on these comfort temperatures. In addition to the resulting neutral, minimal and maximal temperatures, a maximal temperature in unoccupied periods is introduced. Furthermore, due to the unpredictable and short periods of bathroom usage, this zone is generally treated as unoccupied allowing temperature increases at all times. The resulting boundary conditions are given in Table 3.

*Table 3
Thermal boundary conditions for all building zones*

in $^\circ\text{C}$	T_{min}	$T_{neutral}$	$T_{max\ occupied}$	$T_{max\ unoccupied}$
1-zone day	19	21	23.5	25
1-zone night	16	18	19.5	/
bed-rooms	16	18	19.5	23.5
other rooms	19	21	23.5	25
bath-rooms	21	22.5	/	26

The simulation is performed with real weather data (DWD, 2012) for the city of Bottrop (North-Rhine Westphalia, Germany), taking the first 60 days of 2012 into account. In order to produce a signal for the

availability of excess electric energy from renewable energy (RE) generation, a standard load profile (SLP) for household customers and the actual renewable energy generation in North-Rhine Westphalia in the observed days are used. The dynamics of the renewable energy generation based on data from the European Energy Exchange [EEX, 2014] is scaled to an output of 1000 kWh per year to match the SLP, which is normalized in the same way. Thus, both annual electricity demand and renewable energy generation are assumed to be 1000 kWh. This results in an assumed future scenario with a theoretical 100 % renewable demand coverage, if the demand or the generation would be completely flexible. However, the availability and the demand do not always match. Thus, the normalized data sets, both with a time step of 15 minutes, are overlaid and every time the supply is greater than the demand the renewable energy signal (RES) is set to true, otherwise to false.

The control algorithm of this approach endeavours to maximise the usage of renewable energies. Therefore, the algorithm reviews the RES, the building’s occupancy, and current temperature conditions in each zone after every 15 minutes. If the RES signal indicates availability, the zones of the building are heated to the maximal temperatures allowed according to the current occupation profiles. At all other points in time, the temperature of all zones is reduced to the minimal comfort temperature. Figure 2 summarizes the control procedure in a flow chart.

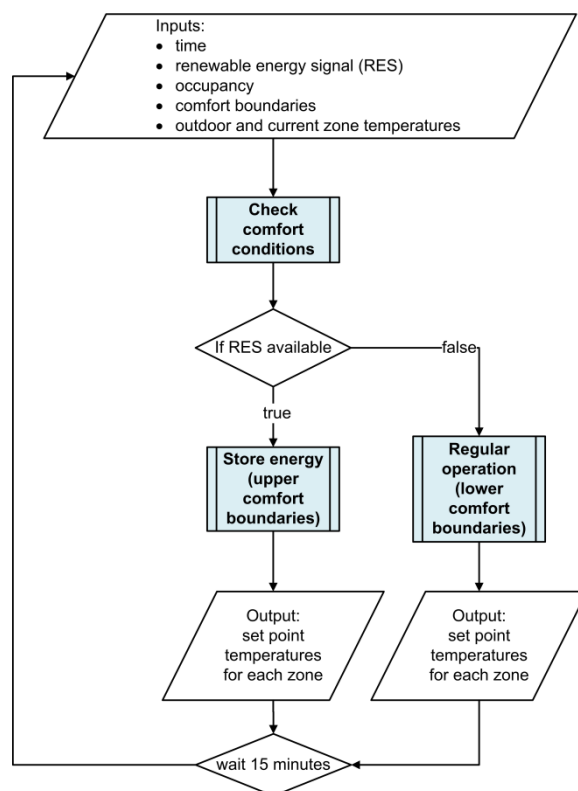


*Figure 2
Flow chart of the developed algorithm*

For this algorithm four scenarios are developed and compared to two reference scenarios, where the heating system is operated in the widespread night-setback mode (regular temperature 21 °C, night-temperature 18 °C, 10 pm until 6 am). The scenarios differ in the subdivision of building zones and the intelligence of the algorithm. The intelligence refers to the forecasting ability of the building’s thermal behaviour. The ‘simple’ version of the algorithm only changes set temperatures when an occupancy change occurs. Whereas the ‘smart’ version stops the energy storage process up to three hours before the expected occupancy of the given zone, depending on the thermal inertia of the observed zone. Furthermore, the ‘smart’ control turns the heating on at a temperature that is 0.5 K higher than the lower comfort limit, while the ‘simple’ version only starts heating when the comfort conditions are violated. Table 4 shows the properties of the four analysed scenarios.

Table 4
Setup of the analysed scenarios

	<i>zones</i>	<i>controller</i>
Reference	single and three separate	night setback
Scenario 1	one single	simple
Scenario 2	one single	smart
Scenario 3	three separate	simple
Scenario 4	three separate	smart

SIMULATION RESULTS

First, the resulting RE signal for the first 60 days of the year 2012 is presented in Figure 3.

Table 5
Energy consumption figures for scenarios 1-4

				S1	S2	S3	S4
energy demand with night-setback	kWh	a		3430			
energy demand with building activation	kWh	b		3950	3890	4390	4450
demand increase	kWh	c	= b - a	520	460	960	1020
demand increase	%	d	= c / a	+ 15	+ 13	+ 28	+ 30
RE consumption with night-setback	kWh	e		1030	(30 %)	1100	(32 %)
RE consumption with building activation	kWh	f		2300	2210	3250	3180
effective consumption within RES	kWh	g	= f - c	1780	1750	2290	2160
effective consumption within RES	%	h	= g / a	52	51	67	63
RE consumption increase / stored RES	kWh	i	= g - e	750	720	1190	1060
RES usage increase	%	j	= i / a	22	21	35	31
storage efficiency	%	k	= i / (f - e)	59	61	55	51



Figure 3

Resulting RES of the scaled renewable generation for the first 60 days of the year 2012

Even though the renewable generation was scaled to exactly the same energy amount as the demand, the availability only matches the demand in approximately 490 hours out of the 1440 hour simulation period. Thus, the building’s heating demand can be covered with renewable energy only at 34 % of the total simulation time.

Within the 60-day simulation period, the two reference buildings with the night-setback heating controller required slightly deviating amounts of energy to keep the temperatures at the desired level. This is due to differences in the precision of calculating inner loads (lights, machines, persons) for single and multi-zone models. For better comprehensibility of the results, the energy demand of the single-zone reference is scaled to the demand of the multi-zone reference, thus to 3430 kWh of thermal energy. Therein, 1030 kWh (30 %) of the total demand, were required during times of true RES for the single-zone reference and 1100 kWh (32 %) for the multi-zone reference respectively. For scenarios one through four, the energy demands, the change in energy demand in comparison to the reference scenarios, and the resulting usage of energy during the RES are given in Table 5. Since the increase of zone temperatures results in generally higher heat demands, the energy storage efficiency is calculated additionally. This index shows the relation between the calculated amount of renewable energy stored within the building structural mass and the resulting additional heat demand, which represents the increased heat losses due to higher zone temperatures.

For better comprehension of the considerable losses due to the activation of the building, the average temperatures in the analysed zones are calculated. These temperatures are calculated separately for day and night time and compared to the average temperatures of the reference system. Table 6 provides the temperature increases in comparison to the reference scenario. Marked in grey are the sections of the table that represent the phases in which the observed zone is assumed usually unoccupied.

Table 6
Average temperature increase in the analysed zones

in °C	1- zone (S1 / S2)	rest-rooms (S3 / S4)	bed-rooms (S3 / S4)	other rooms (S3 / S4)
day	+ 0.5	+ 0.4	+ 1.5	+ 0.6
night	+ 0.5	+ 2.6	+ 0.7	+ 2.5

Since the compliance to comfort conditions is an essential criterion for the analysed algorithm, violations of comfort limits are tracked. Particularly, violations of the upper comfort limits (Table 3) that are induced by the thermal activation of the building are analysed on a 15 min basis. The resulting total violation hours and the share of the simulation time with violations are calculated. Additionally, the average extent (in kelvin) of the upper limit exceedance is calculated. Finally, to quantify the total level of comfort impairment a correlation index for the time and the extent of comfort

violations is introduced. Thus, for all violations their occurrence time (in 15-minute time-steps) is multiplied with the absolute exceedance value (in kelvin). The resulting aggregated index in kelvin hours facilitates the assessment of the violation severity. The detailed results are given in Table 7.

Table 7
Comfort violations and resulting impairment

	S 1	S 2	S 3	S 4
violation time (h)	50	28	112	81
violation time (%)	3.5	1.9	7.8	5.6
Ø violation extent (K)	0.46	0.43	0.65	0.47
impairment index (K·h)	23	12	73	38

In Figure 4, an exemplary plot of the algorithm's temperature control for the 5th through 8th of January in 2012 is given. It shows how the air temperatures were adapted in reaction to the RES signal in the 'other rooms' zone of the 'smart' multi-zone algorithm (Scenario 4). It can be clearly seen how the controller changes the set temperature of the zone in accordance to the availability of RE and the zone's occupancy. On the 5th and 6th of January the temperatures are consequently increased throughout the day, whereas on the 7th and 8th the set temperatures are partially reduced and the building's thermal mass is uncharged.

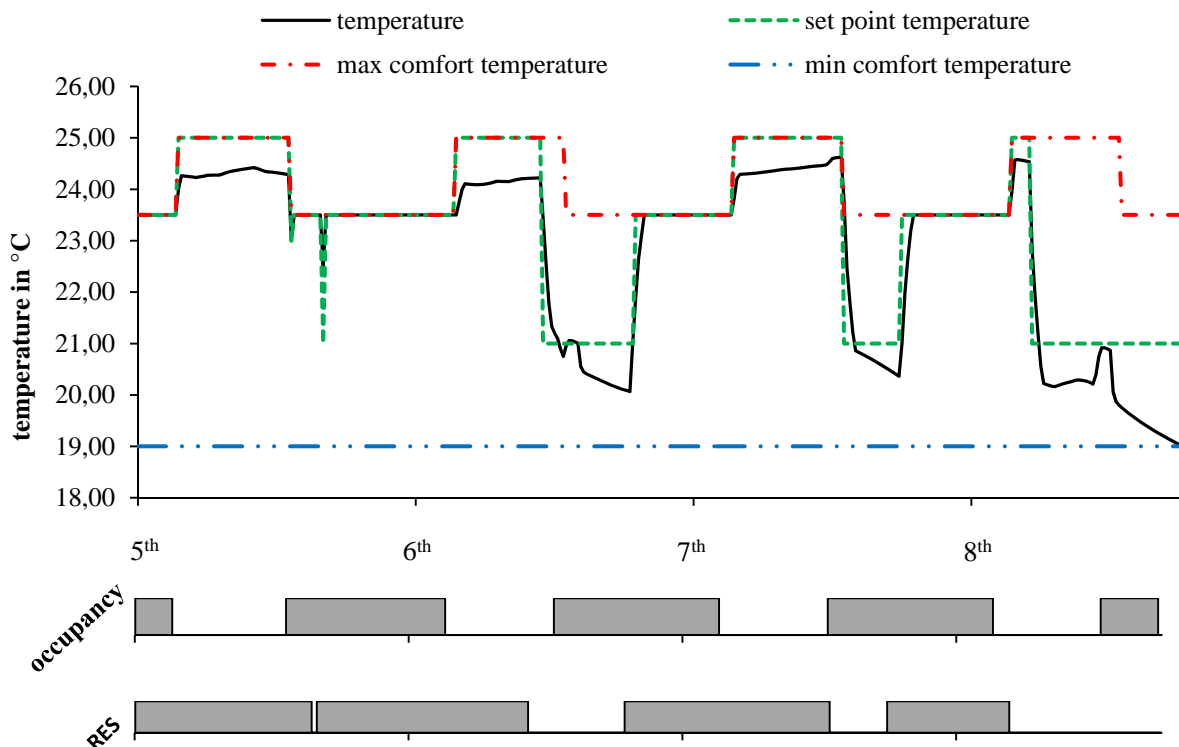


Figure 4
Example of the temperature control in 'other rooms' zone of Scenario 4

DISCUSSION

The analysis shows a clear increase of renewable energy usage due to the usage of the building's structural mass as a storage. Depending on the scenario, energy usage in the periods of RES availability increases by 19 - 35 %. These percentages are related to the basic energy demand of the reference scenario and do not take into account the RE which is used and lost due to the storage process. These losses result from the considerably higher room temperatures through the storage process, as presented in Table 6. As a result, the total demand increases for scenarios S1 and S2 by approximately 14 % and for scenarios S3 and S4 by approximately 29 %. If the stored renewable energy is compared to the demand increase of the building, storage efficiencies of 50 to 60 % are achieved by the building activation.

For a precise evaluation of the consequences of such storage efficiency, detailed economic and ecological boundary conditions are required. Since these future conditions could be only guessed, this analysis focuses on the technological facts of the concept. First, all required additional energy is used during the periods of high RE availability. As a result, the storage process and the resulting losses do not induce additional CO₂ emissions. Second, besides electric thermostat valves and a controller, which could potentially be a cloud service in the future, no further investments are required. And third, if combined with a private photovoltaic system, even a storage with an efficiency lower than 50 % would be economic, if the storage itself is available at no cost. This holds if calculating with the German electricity price (currently 0.30 €/kWh) and the current feed-in tariff (0.12 €/kWh) or the electricity exchange prices (usually in the range of 0.02-0.06 €/kWh) (DESTATIS, 2015).

Nevertheless, even without a detailed economic analysis, it can be expected that there will be conditions when excess renewable energy can be stored more efficiently in centralized large-scale storage systems, battery storage systems or even electrical vehicles in the future. However, the very low cost of the implementation of thermal mass activation in combination with the large and predictable heating energy demand of buildings shows that such an approach has the potential to support the incorporation of fluctuating RE generation in the future energy system.

Still, even if technological potential for this storage approach is detected, the acceptability of the technology and thus the impact upon the residents' comfort is crucial. This analysis shows that the single-zone algorithms have distinctly less comfort violations than the multi-zone controllers do. This is due to the very narrow range of temperatures, which fit all parts of the single-zone. Thus, the controller almost never chooses temperatures, which could possibly violate comfort conditions, even if the building is unoccupied.

Accordingly, for the smart single-zone algorithm just 2 % of the time has comfort violations. The multi-zone algorithm has more flexibility in the choice of set temperatures for the different zones. This, however, results in generally higher temperatures and a higher chance of comfort violations. As shown in Table 6, the average temperature increase of the single-zone is 0.5 K, while the multi-zone algorithm increases zone temperatures by up to 2.5 K. Such temperature increases are only performed when the observed zones are unoccupied. Average increases of less than 0.7 K are observed in occupied zones. Still, especially for the simple version of the controller, the strong increases in unoccupied times lead to comfort violations at almost 8 % of the observed time. However, the smart algorithm is capable of reducing this value to 5.6 %. Furthermore, the observed average extent of the violations, which is on average around 0.5 K, and the defined impairment index indicate that the observed violations are regularly not very severe.

Further evaluation of the results has shown that $\frac{3}{4}$ of all comfort violations occurred in the bedroom zones. This is comprehensible since this zone has the largest delta between the natural temperature, the maximum temperature when occupied and the maximum unoccupied temperature that is used for storing energy. Furthermore, the bedrooms are assumed as unoccupied for 16 hours a day and therefore this zone is strongly charged throughout the day. Additionally, due to the low desired temperatures in this zone, the gradient to the ambient is smaller than within the other zones. Thus, especially when the room temperature is already low, the further cool-down process is significantly extended.

Finally, for the bedrooms the maximum comfort temperature of 19.5 °C, as taken from literature, is very conservative. It can be assumed, that the average comfort violation of just about 0.5 K, leading to temperatures of 20 °C in the bedrooms would be still acceptable at the beginning of the bedroom occupation. Especially, since these slight comfort violations come hand in hand with a distinct increase of energy usage in periods of the RES. While RE integration already increased by 20 % for the single-zone algorithm, it increases more than 30 % for the multi-zone controller. If this excess RE is delivered at a lower price, the residents might be willing to diverge slightly from the typical temperature profiles.

CONCLUSIONS

The presented analysis faced the challenge of matching availability of renewable energies with the heating demand of a residential one-family house. We assumed a scenario, where the total renewable generation matched the energy demand of the observed period. Nevertheless, due to missing coordination of availability and demand only one third of the building's demand was covered through RE.

Therefore, different algorithms, which activate the building's thermal mass at times of high RE availability, were implemented and tested. The analysis has shown that even relatively simple DSM approaches can improve the usage of RE. However, when attempting to reach a RE share higher than 50 % more sophisticated algorithms are required. In this analysis, a multi-zone temperature control with independent occupation profiles and zone-specific temperature ranges was used. This approach allowed doubling the renewable coverage of heating demand, reaching close to 70 % RE usage. This was achieved at the cost of slightly increased comfort violations, especially in the bedroom zone.

The evaluation shows a strong potential for the integration of the building's thermal mass as a thermal storage in DSM activities. Still, it can be also seen that the algorithm is increasing the overall energy demand and potentially reducing indoor comfort in some cases. Therefore, it is crucial to monitor that only renewable energy is used for the activation. Furthermore, depending on the desired extent of energy storage it might be necessary to integrate comfort protection mechanisms in the control algorithm. This can be done through a combination of occupation- and building's thermal behaviour predictions. The algorithm implemented in this analysis was just using a simple static prediction of the cool-down time and managed to keep comfort violations lower than 0.5 K. Thus, it is not even clear whether the detected violations would be indeed realised as a distinct reduction in comfort by the residents.

Future buildings will already have all the required technological components to integrate thermal mass activation and upgrading an existing building with the required components would be still distinctly cheaper than any conventional energy storage. Taking this into account, any extent of structural mass activation will contribute a valuable effect for the coordination of renewable energy generation and heating energy demand. Therein, every building owner could adapt the extent of energy storage according to the desired levels of comfort adherence or RE integration.

In the future, this approach will be further developed including heating systems directly coupled with the buildings structural thermal mass, as floor heating and concrete core activation for example. Such systems require a more sophisticated state analysis and prediction of the thermal mass temperature as well as a solid demand prediction. However, they have even larger potential to store large amounts of energy without a strong increase in the temperatures within the building. Furthermore, an experimental analysis of the comfort perception of such dynamic room- and radiation-temperature changes as induced by the thermal mass activation will be performed. Finally, it is intended to develop a control algorithm that integrates RE predictions, demand predictions, and occupancy

predictions to control several heating and mass activation technologies within the building.

ACKNOWLEDGEMENT

Grateful acknowledgement is made for the financial support by E.ON gGmbH.

REFERENCES

- BMWi, Federal Ministry for Economic Affairs and Energy (2013). "Energy Consumption Surveys – 'Endenergieverbrauch nach Anwendungsbereichen' ". Berlin.
- DESTATIS, Federal Statistical Office (2015). "Preise - Daten zur Energiepreisentwicklung" Available: <https://www.destatis.de/DE/ZahlenFakten/GesamtwirtschaftUmwelt/Preise/Preise.html>. [accessed: 03.2015]
- DIN, Deutsches Institut für Normung e. V. (2006). „DIN EN ISO 7730, 2006-05: Ergonomics of the thermal environment - Analytical determination and interpretation of thermal comfort using calculation of the PMV and PPD indices and local thermal comfort criteria.”
- DIN, Deutsches Institut für Normung e. V. (2012). „DIN EN 12831, 2003-08: Heating systems in buildings - Method for calculation of the design heat load.”
- DWD, Deutscher Wetterdienst (2012). "Klima und Umwelt – Klimadaten". Available: <http://www.dwd.de/>. [accessed: 10.07.2014].
- EEX, European Energy Exchange (2014). "Market Data." Available: http://www.eex.com/en/Market_Data. [accessed: 07-12.2014].
- Lauster, Moritz, et al. (2014). "Low Order Thermal Network Models for Dynamic Simulations of Buildings on City District Scale." Building and Environment, Volume 73, pp. 223-231.
- Modelica Association et al. (2014). "Modelica and the Modelica Association". Available: <https://www.modelica.org/>. [accessed: 10.07.2014].
- Peeters, Leen et al. (2009). "Thermal comfort in residential buildings: Comfort values and scales for building energy simulation." In Applied Energy 86 (5), pp. 772-780. DOI: 10.1016/j.apenergy.2008.07.011.
- VDI, The Association of German Engineers (2012). "Guideline 6007, Part 1: Calculation of transient thermal response of rooms and buildings - Modelling of rooms."
- Wolisz, Henryk, et al. (2013). "Dynamic Simulation of Thermal Capacity and Charging/Discharging Performance for Sensible Heat Storage in Building Wall Mass." Proceedings of IBPSA Building Simulation Conference 2013.